



Quasiparticle coherence in the nematic state of FeSe

H. Pfau ^{1,2,3,*} M. Yi,⁴ M. Hashimoto,⁵ T. Chen,⁴ P.-C. Dai ⁴ Z.-X. Shen,^{1,6,7} S.-K. Mo,² and D. Lu⁵

¹Stanford Institute of Materials and Energy Science, SLAC National Accelerator Laboratory, Menlo Park, California 94025, USA

²Advanced Light Source, Lawrence Berkeley National Laboratory, Berkeley, California 94720, USA

³Department of Physics, The Pennsylvania State University, University Park, Pennsylvania 16802, USA

⁴Department of Physics and Astronomy, Rice University, Houston, Texas 77005, USA

⁵Stanford Synchrotron Radiation Lightsource, SLAC National Accelerator Laboratory, Menlo Park, California 94025, USA

⁶Department of Physics, Stanford University, Stanford, California 94305, USA

⁷Geballe Laboratory for Advanced Materials, Department of Applied Physics, Stanford University, Stanford, California 94305, USA



(Received 16 June 2021; accepted 8 November 2021; published 2 December 2021)

Electronic nematicity is a ubiquitous phenomenon in iron-based superconductors but its origin is still debated. Most models consider either spin or orbital degrees of freedom as the driving force but typically do not take electronic correlations into account. However, mass enhancements, coherent-incoherent crossovers, and the strong orbital differentiation can only be understood using correlations in a Hund's metal framework. Here, we study the influence of nematicity on the quasiparticle coherence in detwinned FeSe using angle-resolved photoemission spectroscopy (ARPES). We compare photoemission spectral weight from d_{xz} and d_{yz} orbitals in the coherent quasiparticle peak and in the incoherent Hubbard band and find an anisotropy between the two orbitals. We interpret our observation in terms of a more coherent d_{xz} orbital compared to the d_{yz} orbital inside the nematic phase. This result is in contrast to earlier predictions of an incoherent d_{xz} orbital and highlights the importance of electronic correlations in the description of nematicity.

DOI: [10.1103/PhysRevB.104.L241101](https://doi.org/10.1103/PhysRevB.104.L241101)

The nematic phase transition breaks the rotational symmetry and is a ubiquitous phenomenon in iron-based superconductors (FeSCs). While it has been studied extensively, the origin of nematicity is still debated. There are plenty of experimental evidences that nematicity is an electronic instability that induces an anisotropy in the B_{2g} channel with respect to the lattice, spin, and orbital degrees of freedom [1–6]. Many of these properties can successfully be described by either an Ising-spin nematic order as a precursor to stripe magnetism [5,7–9] or by orbital order in the form of ferro-orbital order or bond order [10–16].

These approaches typically do not take electronic correlations from local interactions into account. However, many experimental and theoretical investigations highlight the importance of correlations in FeSCs [17–24]. The interplay of Coulomb interactions, Hund's rule coupling, and the multi-orbital nature place FeSCs into a strongly correlated metal regime often called Hund's metal. It is responsible for the bad metallic behavior with an overall suppression of quasiparticle coherence but in a strongly orbital-dependent fashion.

FeSe is an important member of the FeSC regarding both its nematic phase and its correlation strength [6]. It is one of the most correlated FeSCs with a large orbital-dependent mass enhancement [25–27], an orbital-dependent coherent-incoherent crossover [23], and high-energy incoherent spectral features observed by ARPES and identified as Hubbard bands [28,29]. FeSe orders nematically below $T_{\text{nem}} = 90$ K but long-range magnetic order is absent [30]. It

is therefore a prime candidate to study nematicity unperturbed by magnetism. Specifically, the nematic band splitting between the d_{xz} and d_{yz} orbitals has been studied extensively by ARPES in this material [26,27,31–39]. FeSe becomes superconducting (SC) below 9 K [40]. Its anisotropic gap function [41–43] could only be explained using models that include some sort of orbital differentiation [43–47]. For example, a strongly different quasiparticle coherence of the d_{xz} and d_{yz} orbitals was proposed to explain the quasiparticle interference pattern and the SC gap structure. [43,48].

While some recent theoretical studies explore the interplay of nematicity and correlations [44,45,47,49,50], experimental evidence is scarce. In particular, there is no clear evidence for an anisotropy of coherence of the d_{xz} and d_{yz} orbitals due to nematicity. Optical spectroscopy studies found an anisotropic Drude weight in the nematic state [51–53] but suffer from an orbital-integrated nature. Quasiparticle interference measurements rely on supporting model calculations for the interpretation of the data in terms of coherence effects [48]. Recent ARPES studies found an anisotropy of the quasiparticle spectral weight between d_{xz} and d_{yz} orbitals in FeSe and BaFe_2As_2 [54,55]. While complications due to photoemission matrix elements and temperature-dependent changes in coherence could be alleviated in Ref. [55], unclear contributions from mixing between Fe $3d$ and Se/As $4p$ orbitals still prevented a clear attribution to correlation effects.

Here, we present ARPES measurements on detwinned FeSe inside the nematic phase. As a key difference to previous studies, we perform a spectral weight analysis not only of the coherent quasiparticle peak but also of the incoherent Hubbard bands. The spectral weight ratio between the two is a

*heike.pfau@psu.edu

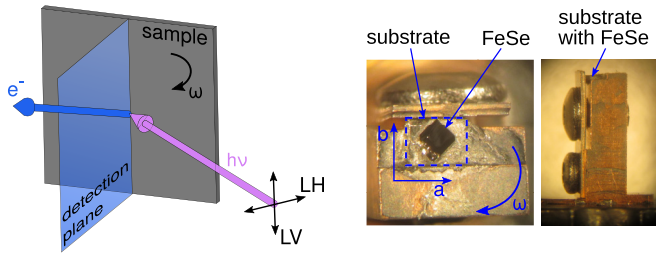


FIG. 1. Experimental geometry of the ARPES measurement. Left: Horizontally (LH) or vertically (LV) polarized light photoemits electrons from the sample. The ARPES analyzer slit selects only those electrons emitted along the detection plane. Azimuthal rotation ω of the sample holder then allows the separate measurement of spectra along k_x and k_y . Right: Photograph of detwinning device.

direct measure of the quasiparticle coherence. Careful experimental procedures allow us to compare the spectral weight between spectra taken along orthogonal momentum directions probing either d_{xz} or d_{yz} orbitals. Our study therefore allows us to directly and unambiguously determine the anisotropy of the quasiparticle coherence between the d_{xz} and d_{yx} orbital. We observe that the d_{xz} orbital has a larger spectral weight in the quasiparticle peak and a smaller spectral weight in the Hubbard band compared to the d_{yz} orbital. We conclude that the d_{xz} orbital is more coherent than the d_{yz} orbital. Since both are degenerate above T_{nem} , this anisotropy is caused by nematic order. The sign of the effect is opposite to previous proposals that suggested a very incoherent d_{xz} orbital [43,48].

High-quality single crystals of FeSe were grown using chemical vapor transport methods [56]. ARPES measurements were performed at SSRL beamline 5-2 with an energy and angular resolution of 18 meV and 0.1° . The samples are cleaved *in situ* and studied at a temperature of 12 K and a base pressure below 5×10^{-11} torr.

The crystals are mounted on a substrate and detwinned with a mechanical clamp as described in [27,31] and shown in Fig. 1. We confirmed that the studied region of the sample surface is fully detwinned using spectra taken with linear horizontal (LH) polarized light (see [57], Fig. S1). The stress necessary to detwin the sample is small enough to prevent a detectable change in dispersion [3,27]. Azimuthal rotation of the sample by 90° selects the momentum directions k_x and k_y of the spectra (Fig. 1). To ensure that we can reliably compare the photoemission intensities between these two spectra, we employ the following procedures. We use a small photon beam spot size of $56 \mu\text{m} \times 26 \mu\text{m}$ and carefully map the sample surface before and after rotation in order to probe the same surface region for both directions. Each spectrum is normalized by its photoemission intensity above the Fermi level integrated between (0.2,0.3) eV. The careful sample alignment and accounting of photon beam current fluctuations limit the variation of this normalization factor to less than 2%. Standard detector nonlinearities and anisotropies are characterized and removed from the spectra using separate measurements on polycrystalline gold.

We use a photon energy of 70 eV, which probes a k_z close to Γ [26]. In addition, the photoemission cross section of Fe 3d relative to Se 4p electrons is enhanced compared to lower photon energies [58] (see also [57], Fig. S2). To study the

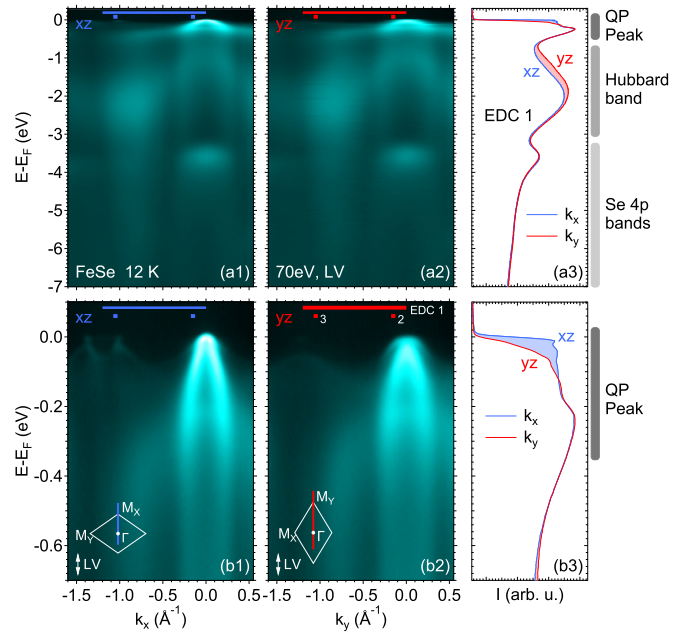


FIG. 2. ARPES spectra of FeSe at 12 K. (a1) Spectrum taken along k_x . (a2) Spectrum taken along k_y . (a3) EDCs obtained from (a1) and (a2) integrated between $k = (0, -1.2) \text{ \AA}^{-1}$ as indicated by the bars on the top of the spectra. (b) same as (a) but zoomed into a smaller energy window close to E_F . Sketches in (b1) and (b2) indicate the measurement directions in the BZ and the orientation of the LV light polarization. The dominantly probed Fe 3d orbital character (xz , yz) is indicated in each panel. Bars on top of the spectra show the momentum integration window for the EDCs discussed in (a3) and (b3) (EDC 1) and in Figs. 3 (EDC 2) and 4 (EDC 3).

spectral weight anisotropy between d_{xz} and d_{yz} , we choose linear vertical (LV) polarized light. This polarization probes the Fe $3d_{xz}$ (d_{yz}) orbital along k_x (k_y) when we select the momentum direction by azimuthal sample rotation (Fig. 1). Away from normal emission, electrons with other orbital character, in particular d_{z^2} , will also contribute to the photoemission intensity but importantly clear selection rules for d_{xz} and d_{yz} are maintained along k_x and k_y [55]. Comparing spectra taken along k_x and k_y will therefore give us direct information about the anisotropy between the d_{xz} and d_{yz} orbitals.

Figures 2(a1) and 2(a2) present our ARPES spectra. Corresponding energy distribution curves (EDCs) integrated between the Brillouin zone (BZ) center Γ and the BZ corners $M_{X,Y}$ are shown in Fig. 2(a3). The large energy window of 7 eV covers three distinct regions, which have been observed and identified in previous ARPES studies combined with dynamical mean-field theory calculations [28,29,59]: (1) A quasiparticle peak predominantly from Fe 3d lies close to the Fermi energy E_F . (2) The broad peak around -2 eV originates from electronic correlations. It was identified as a Hubbard band of iron and we will follow this nomenclature here. (3) The region between -4 and -7 eV covers the Se 4p bands, the intensity of which is suppressed as mentioned above. Figure 2(b) presents a zoom into the energy window around the quasiparticle peak close to E_F . The overall structure of the spectrum is the same along k_x and k_y and it agrees well with the earlier reports. However, a direct comparison

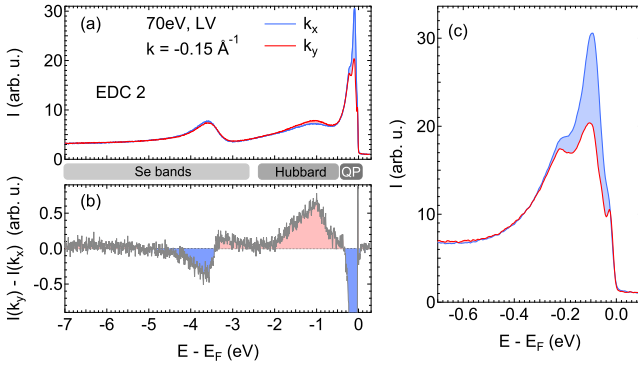


FIG. 3. Comparison of EDCs along k_x and k_y taken close to Γ . The momentum integration window for the EDCs is indicated in Fig. 2 with the label EDC 2. (a) EDCs shown in the whole measured energy window. (b) Difference of intensity I between the two EDCs shown in (a). We limit the displayed range on the vertical axis in order to highlight anisotropies around the Hubbard band located around -1 eV. The signature of the quasiparticle peak is therefore cut off in this plot. (c) Zoom of (a) into smaller energy scales close to the Fermi level to highlight anisotropies in the quasiparticle spectral weight of the hole bands.

of the integrated EDCs between both momentum directions reveals an anisotropic spectral weight distribution. Specifically, the Hubbard band has a larger, and the quasiparticle peak a smaller spectral weight along k_y compared to k_x . In contrast, the energy region dominated by Se $4p$ bands shows no difference.

In order to gain insights into the momentum dependence of this effect, we analyze two representative EDCs close to Γ and M in Figs. 3 and 4. They separately probe the behavior of the hole and the electron band. We show in Supplemental Material, Fig. S3 that we obtain the same result over the whole

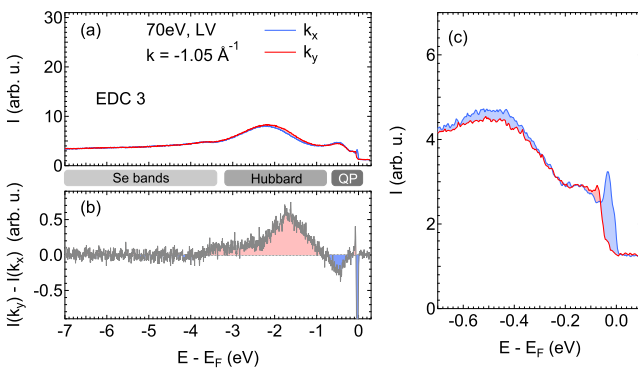


FIG. 4. Comparison of EDCs along k_x and k_y taken close to M_X and M_Y . The momentum integration window for the EDCs is indicated in Fig. 2 with the label EDC 3. (a) EDCs shown in the whole measured energy window. (b) Difference of intensity I between the two EDCs shown in (a). We limit the displayed range on the vertical axis in order to highlight anisotropies around the Hubbard band located around -2 eV. The signature of the quasiparticle peak is therefore cut off in this plot. (c) Zoom of (a) into smaller energy scales close to the Fermi level to highlight anisotropies in the quasiparticle spectral weight of the electron bands.

momentum range [57]. Figure 3(a) compares the EDCs at $k_x = k_y = -0.15 \text{ \AA}^{-1}$. At this momentum the quasiparticle peak is not cut off by the Fermi edge and fully visible. In order to better visualize the spectral weight anisotropy, we plot the difference of the intensity between the two momentum directions in Fig. 3(b) and a zoom into the low-energy region close to the quasiparticle peak in Fig. 3(c). We use the same method in Fig. 4 for the EDCs at $k_x = k_y = -1.05 \text{ \AA}^{-1}$ close to the BZ corner. For both momenta, we find the same behavior as for the integrated EDC in Fig. 2. The Hubbard band has a larger spectral weight along k_y than k_x while the quasiparticle peak has a smaller spectral weight. We find no difference at large energies in the region of the Se $4p$ bands. The only difference between Γ and M is a peak in the EDC at -3.5 eV in Fig. 3(a). It lies close to the top of the Se bands and was interpreted as Fe $3d_{xz/yz}$ spectral weight mixed into these bands [29]. From the difference plot in Fig. 3(b) it becomes clear that the integrated spectral weight of this peak between $(-2.5, -4.5)$ eV changes only slightly between k_x and k_y and the peak mainly shifts its position.

According to the photoemission selection rules, our main observation implies that the d_{xz} orbital has a larger quasiparticle spectral weight and a smaller spectral weight in the Hubbard band compared to the d_{yz} orbital. Se $4p$ orbital admixture does not contribute to this spectral weight anisotropy, since the spectra remain unchanged at high energies. Since both orbitals are degenerate in the tetragonal state above the nematic transition temperature, the anisotropy at low temperature is due to the lifting of this degeneracy by nematic order. Our observations indicate that spectral weight is transferred between the coherent part of the spectrum (the quasiparticle peak) and the incoherent part of the spectrum (the Hubbard band) due to nematicity. Therefore, we conclude that electrons with d_{xz} orbital character are more coherent than those with d_{yz} character inside the nematic state. We note that the energy-integrated spectral weight of the EDCs is different along the two momentum directions. Since we only probe occupied states, we expect spectral weight to be transferred also above the Fermi level.

The difference in coherence can be understood within the idea of orbital differentiation: When the degeneracy of d_{xz} and d_{yz} is lifted, not only will their binding energies become different but also their coherence. Recent theoretical calculations of the quasiparticle self-energy found that the lifted orbital degeneracy indeed leads to different coherence factors Z of the d_{xz} and d_{yz} orbitals [36,45,49]. Their hierarchy depends on the precise form of the nematic perturbation. Since it requires certain assumptions to extract the quasiparticle self-energies from ARPES spectra, a theoretical evaluation of both the high and low-frequency intensity of the spectral function is desirable. Such a comparison may enable the identification of important ingredients for a microscopic theory of nematicity in particular the role of Coulomb interaction and Hund's rule coupling.

To provide an estimate for the size of the spectral weight anisotropy, we integrate the spectral weight in the energy region of the Hubbard band for each EDC and obtain an anisotropy between 2% and 5% for the three cases shown in Figs. 2–4. For the quasiparticle peak, which is not cut

off by the Fermi energy only for the EDCs in Fig. 3, we obtain -16% . The size of the anisotropy is likely momentum dependent [55]. We do not consider any background contribution in this analysis and the estimates should be taken as lower bounds.

Our results are in agreement with previous strain-dependent ARPES studies in BaFe_2As_2 that report an anisotropic quasiparticle spectral weight with the same sign [55]. Orbital-dependent correlations are therefore very likely the origin in both materials. In contrast, earlier proposals of a very incoherent d_{xz} orbital inside the nematic state of FeSe [43,48] are incompatible with our result. The main purpose of the phenomenological approach in Refs. [43,48] was to remove the d_{xz} spectral weight of the electron band from the Fermi level to explain the Fermi surface inside the nematic state and the SC gap structure. There are several alternative proposals that lead to a similar effect without invoking incoherence [27,36,46,47,60].

A recent theoretical study demonstrated that SC order is boosted in Hund's metals [61]. An important ingredient is the finite frequency contributions from the spectral weight that is redistributed in a window of J_H around E_F typical for Hund's metals. Our results demonstrate that the spectral weight exactly in this energy window becomes anisotropic due to nematicity and we speculate that this will influence the SC properties of FeSe. At the same time, the question arises whether correlations can also boost nematicity and need to be taken into account in microscopic models.

In summary, we studied the quasiparticle coherence of the d_{xz} and d_{yz} orbital in detwinned FeSe inside the nematic phase

using ARPES. We compare the spectral weight in the quasiparticle peak, in the Hubbard band and in the energy region of the Se $4p$ bands for two spectra probing the d_{xz} and d_{yz} orbital character, respectively. We find that the Hubbard band has a smaller, and the quasiparticle peak a larger spectral weight for the d_{xz} orbital while their spectral weight contribution to the Se bands remains the same. Our results imply that the d_{xz} orbital is more coherent than the d_{yz} orbital. Our result is in agreement with earlier studies on strained BaFe_2As_2 and suggests a common origin rooted in the correlated nature of FeSC. It calls for a better theoretical understanding of the interplay of nematicity and Hund's metal physics.

We are very grateful for valuable discussions with Brian Anderson, Lara Benfatto, Massimo Capone, Laura Fanfarillo, Peter Hirschfeld and Andreas Kreisel. H.P. acknowledges support from the German Science Foundation (DFG) under reference PF 947/1-1. This work was supported by the Department of Energy, Office of Basic Energy Sciences, under Contract No. DE-AC02-76SF00515. Use of the Stanford Synchrotron Radiation Lightsource, SLAC National Accelerator Laboratory, is supported by the U.S. Department of Energy, Office of Science, Office of Basic Energy Sciences under Contract No. DE-AC02-76SF00515. Work at Lawrence Berkeley National Laboratory was funded by the U.S. Department of Energy, Office of Science, Office of Basic Energy Sciences under Contract No. DE-AC02-05-CH11231. The FeSe single crystal growth and characterization work at Rice was supported by the U.S. DOE, BES DE-SC0012311 and in part by the Robert A. Welch Foundation Grant No. C-1839 (P.D.).

-
- [1] D. C. Johnston, *Adv. Phys.* **59**, 803 (2010).
 [2] J. Paglione and R. L. Greene, *Nat. Phys.* **6**, 645 (2010).
 [3] I. R. Fisher, L. Degiorgi, and Z. X. Shen, *Rep. Prog. Phys.* **74**, 124506 (2011).
 [4] J.-H. Chu, H.-H. Kuo, J. G. Analytis, and I. R. Fisher, *Science* **337**, 710 (2012).
 [5] R. M. Fernandes, A. V. Chubukov, and J. Schmalian, *Nat. Phys.* **10**, 97 (2014).
 [6] A. E. Böhmer and A. Kreisel, *J. Phys.: Condens. Matter* **30**, 023001 (2017).
 [7] C. Fang, H. Yao, W.-F. Tsai, J. P. Hu, and S. A. Kivelson, *Phys. Rev. B* **77**, 224509 (2008).
 [8] C. Xu, M. Müller, and S. Sachdev, *Phys. Rev. B* **78**, 020501(R) (2008).
 [9] R. M. Fernandes, A. V. Chubukov, J. Knolle, I. Eremin, and J. Schmalian, *Phys. Rev. B* **85**, 024534 (2012).
 [10] W. Lv, J. Wu, and P. Phillips, *Phys. Rev. B* **80**, 224506 (2009).
 [11] C.-C. Lee, W.-G. Yin, and W. Ku, *Phys. Rev. Lett.* **103**, 267001 (2009).
 [12] C.-C. Chen, J. Maciejko, A. P. Sorini, B. Moritz, R. R. P. Singh, and T. P. Devereaux, *Phys. Rev. B* **82**, 100504(R) (2010).
 [13] S. Onari and H. Kontani, *Phys. Rev. Lett.* **109**, 137001 (2012).
 [14] A. V. Chubukov, M. Khodas, and R. M. Fernandes, *Phys. Rev. X* **6**, 041045 (2016).
 [15] Y. Su, H. Liao, and T. Li, *J. Phys.: Condens. Matter* **27**, 105702 (2015).
 [16] K. Jiang, J. Hu, H. Ding, and Z. Wang, *Phys. Rev. B* **93**, 115138 (2016).
 [17] K. Haule and G. Kotliar, *New J. Phys.* **11**, 025021 (2009).
 [18] Z. P. Yin, K. Haule, and G. Kotliar, *Nat. Mater.* **10**, 932 (2011).
 [19] L. de' Medici, G. Giovannetti, and M. Capone, *Phys. Rev. Lett.* **112**, 177001 (2014).
 [20] K. M. Stadler, G. Kotliar, A. Weichselbaum, and J. von Delft, *Ann. Phys.* **405**, 365 (2019).
 [21] L. de' Medici, J. Mravlje, and A. Georges, *Phys. Rev. Lett.* **107**, 256401 (2011).
 [22] M. Yi, Y. Zhang, Z.-X. Shen, and D. Lu, *npj Quantum Mater.* **2**, 57 (2017).
 [23] M. Yi, Z.-K. Liu, Y. Zhang, R. Yu, J.-X. Zhu, J. Lee, R. Moore, F. Schmitt, W. Li, S. Riggs *et al.*, *Nat. Commun.* **6**, 7777 (2015).
 [24] F. Hardy, A. E. Böhmer, D. Aoki, P. Burger, T. Wolf, P. Schweiss, R. Heid, P. Adelmann, Y. X. Yao, G. Kotliar, J. Schmalian, and C. Meingast, *Phys. Rev. Lett.* **111**, 027002 (2013).
 [25] J. Malet, V. B. Zabolotnyy, D. V. Evtushinsky, S. Thirupathaiah, A. U. B. Wolter, L. Harnagea, A. N. Yaresko, A. N. Vasiliev, D. A. Chareev, A. E. Böhmer *et al.*, *Phys. Rev. B* **89**, 220506(R) (2014).
 [26] M. D. Watson, T. K. Kim, A. A. Haghighirad, N. R. Davies, A. McCollam, A. Narayanan, S. F. Blake, Y. L. Chen, S. Ghannadzadeh, A. J. Schofield *et al.*, *Phys. Rev. B* **91**, 155106 (2015).

- [27] M. Yi, H. Pfau, Y. Zhang, Y. He, H. Wu, T. Chen, Z. R. Ye, M. Hashimoto, R. Yu, Q. Si *et al.*, *Phys. Rev. X* **9**, 041049 (2019).
- [28] D. V. Evtushinsky, M. Aichhorn, Y. Sassa, Z. H. Liu, J. Maletz, T. Wolf, A. N. Yaresko, S. Biermann, S. V. Borisenko, and B. Buchner, [arXiv:1612.02313](https://arxiv.org/abs/1612.02313).
- [29] M. D. Watson, S. Backes, A. A. Haghighirad, M. Hoesch, T. K. Kim, A. I. Coldea, and R. Valentí, *Phys. Rev. B* **95**, 081106(R) (2017).
- [30] T. M. McQueen, A. J. Williams, P. W. Stephens, J. Tao, Y. Zhu, V. Ksenofontov, F. Casper, C. Felser, and R. J. Cava, *Phys. Rev. Lett.* **103**, 057002 (2009).
- [31] H. Pfau, S. D. Chen, M. Yi, M. Hashimoto, C. R. Rotundu, J. C. Palmstrom, T. Chen, P.-C. Dai, J. Straquadine, A. Hristov *et al.*, *Phys. Rev. Lett.* **123**, 066402 (2019).
- [32] M. D. Watson, A. A. Haghighirad, L. C. Rhodes, M. Hoesch, and T. K. Kim, *New J. Phys.* **19**, 103021 (2017).
- [33] Y. Zhang, M. Yi, Z.-K. Liu, W. Li, J. J. Lee, R. G. Moore, M. Hashimoto, M. Nakajima, H. Eisaki, S.-K. Mo *et al.*, *Phys. Rev. B* **94**, 115153 (2016).
- [34] M. D. Watson, T. K. Kim, L. C. Rhodes, M. Eschrig, M. Hoesch, A. A. Haghighirad, and A. I. Coldea, *Phys. Rev. B* **94**, 201107(R) (2016).
- [35] A. Fedorov, A. Yaresko, T. K. Kim, Y. Kushnirenko, E. Haubold, T. Wolf, M. Hoesch, A. Grüneis, B. Büchner, and S. V. Borisenko, *Sci. Rep.* **6**, 36834 (2016).
- [36] L. Fanfarillo, J. Mansart, P. Toulemonde, H. Cercellier, P. Le Fèvre, F. Bertran, B. Valenzuela, L. Benfatto, and V. Brouet, *Phys. Rev. B* **94**, 155138 (2016).
- [37] Y. Suzuki, T. Shimojima, T. Sonobe, A. Nakamura, M. Sakano, H. Tsuji, J. Omachi, K. Yoshioka, M. Kuwata-Gonokami, T. Watashige *et al.*, *Phys. Rev. B* **92**, 205117 (2015).
- [38] T. Shimojima, Y. Suzuki, T. Sonobe, A. Nakamura, M. Sakano, J. Omachi, K. Yoshioka, M. Kuwata-Gonokami, K. Ono, H. Kumigashira *et al.*, *Phys. Rev. B* **90**, 121111(R) (2014).
- [39] K. Nakayama, Y. Miyata, G. N. Phan, T. Sato, Y. Tanabe, T. Urata, K. Tanigaki, and T. Takahashi, *Phys. Rev. Lett.* **113**, 237001 (2014).
- [40] F.-C. Hsu, J.-Y. Luo, K.-W. Yeh, T.-K. Chen, T.-W. Huang, P. M. Wu, Y.-C. Lee, Y.-L. Huang, Y.-Y. Chu, D.-C. Yan, and M.-K. Wu, *Proc. Natl. Acad. Sci. USA* **105**, 14262 (2008).
- [41] H. C. Xu, X. H. Niu, D. F. Xu, J. Jiang, Q. Yao, Q. Y. Chen, Q. Song, M. Abdel-Hafiez, D. A. Chareev, A. N. Vasiliev *et al.*, *Phys. Rev. Lett.* **117**, 157003 (2016).
- [42] D. Liu, C. Li, J. Huang, B. Lei, L. Wang, X. Wu, B. Shen, Q. Gao, Y. Zhang, X. Liu, Y. Hu, Y. Xu, A. Liang, J. Liu, P. Ai, L. Zhao, S. He, L. Yu, G. Liu, Y. Mao *et al.*, *Phys. Rev. X* **8**, 031033 (2018).
- [43] P. O. Sprau, A. Kostin, A. Kreisel, A. E. Böhmer, V. Taufour, P. C. Canfield, S. Mukherjee, P. J. Hirschfeld, B. M. Andersen, and J. C. S. Davis, *Science* **357**, 75 (2017).
- [44] H. Hu, R. Yu, E. M. Nica, J.-X. Zhu, and Q. Si, *Phys. Rev. B* **98**, 220503(R) (2018).
- [45] R. Yu, J.-X. Zhu, and Q. Si, *Phys. Rev. Lett.* **121**, 227003 (2018).
- [46] J. Kang, R. M. Fernandes, and A. Chubukov, *Phys. Rev. Lett.* **120**, 267001 (2018).
- [47] L. Benfatto, B. Valenzuela, and L. Fanfarillo, *npj Quantum Mater.* **3**, 56 (2018).
- [48] A. Kostin, P. O. Sprau, A. Kreisel, Y. X. Chong, A. E. Böhmer, P. C. Canfield, P. J. Hirschfeld, B. M. Andersen, and J. C. S. Davis, *Nat. Mater.* **17**, 869 (2018).
- [49] L. Fanfarillo, G. Giovannetti, M. Capone, and E. Bascones, *Phys. Rev. B* **95**, 144511 (2017).
- [50] D. Steffensen, A. Kreisel, P. J. Hirschfeld, and B. M. Andersen, *Phys. Rev. B* **103**, 054505 (2021).
- [51] C. C. Homes, T. Wolf, and C. Meingast, *Phys. Rev. B* **102**, 155135 (2020).
- [52] M. Chinotti, A. Pal, L. Degiorgi, A. E. Böhmer, and P. C. Canfield, *Phys. Rev. B* **98**, 094506 (2018).
- [53] C. Mirri, A. Dusza, S. Bastelberger, M. Chinotti, L. Degiorgi, J.-H. Chu, H.-H. Kuo, and I. R. Fisher, *Phys. Rev. Lett.* **115**, 107001 (2015).
- [54] C. Cai, T. T. Han, C. G. Wang, L. Chen, Y. D. Wang, Z. M. Xin, M. W. Ma, Y. Li, and Y. Zhang, *Chin. Phys. B* **29**, 077401 (2020).
- [55] H. Pfau, S. D. Chen, M. Hashimoto, N. Gauthier, C. R. Rotundu, J. C. Palmstrom, I. R. Fisher, S.-K. Mo, Z.-X. Shen, and D. Lu, *Phys. Rev. B* **103**, 165136 (2021).
- [56] A. E. Böhmer, V. Taufour, W. E. Straszheim, T. Wolf, and P. C. Canfield, *Phys. Rev. B* **94**, 024526 (2016).
- [57] See Supplemental Material at <http://link.aps.org/supplemental/10.1103/PhysRevB.104.L241101> for data in LH polarization, data taken with different photon energies and a detailed momentum dependent analysis of the spectral weight.
- [58] J. Yeh and I. Lindau, *At. Data Nucl. Data Tables* **32**, 1 (1985).
- [59] J. Huang, R. Yu, Z. Xu, J.-X. Zhu, Q. Jiang, M. Wang, H. Wu, T. Chen, J. D. Denlinger, S.-K. Mo *et al.*, [arXiv:2010.13913](https://arxiv.org/abs/2010.13913).
- [60] L. C. Rhodes, J. Böker, M. A. Müller, M. Eschrig, and I. M. Eremin, *npj Quantum Mater.* **6**, 45 (2021).
- [61] L. Fanfarillo, A. Valli, and M. Capone, *Phys. Rev. Lett.* **125**, 177001 (2020).